TRUE-AMPLITUDE CRS-BASED KIRCHHOFF TIME MIGRATION FOR AVO ANALYSIS

Miriam Spinner

email: *Miriam.Spinner@gpi.uka.de*
keywords: *seismics, imaging, CRS, migration, AVO, AVA*

ABSTRACT

So far, CRS-based limited aperture migration has mainly been introduced to increase the efficiency of Kirchhoff depth migration and to reduce aperture-related artefacts. However, the size of the migration aperture does not only influence the achievable image quality but does also strongly impact the reliability of the migration amplitudes. By transferring the minimum aperture migration approach to the time domain, a consistent workflow can be set up that leads to an improved input for AVO/AVA analyses.

INTRODUCTION

The Common-Reflection-Surface (CRS) stack method as highly automated imaging process has been successfully applied to various data sets. Its implementation for zero-offset (ZO) simulation was initially mainly considered as an alternative to stacking procedures like normal moveout/dip moveout (NMO/DMO)/ stack. Meanwhile, the stacking parameters of the CRS stack, the so-called kinematic wavefield attributes, grow more and more important as they provide additional informations that can be utilized in following processing steps.

Jäger (2005) employed the CRS attributes in pre- and poststack Kirchhoff depth migration to estimate the size and location of the minimum migration aperture. His primary aim was to improve the migrated image by reducing migration artifacts and avoiding operator aliasing. In addition, the efficiency of the migration process considerably increased. Besides these kinematic aspects, the aperture size also strongly influences the quality of the migration amplitudes. Schleicher et al. (1997) showed that optimum amplitude behavior is obtained for restricting the migration aperture to the size of the projected Fresnel zone. The advantages of minimum-aperture migration with respect to the amplitudes are also obvious from Figure 1: in conventional migration (Figure 1a) the stationary point where the operator is tangent to the event and the projected Fresnel zone are unknown prior to migration. Thus, the aperture has to be centered around the operator's apex; its size is usually user-given. Choosing the aperture too small leads to the loss of steep events, if the aperture size even falls below the size of the projected Fresnel zone the amplitudes become meaningless. On the other hand, too big an aperture means that a lot of noise off the event and possibly other events contribute to the diffraction stack and deteriorate the amplitudes. In addition, the risk of operator aliasing is increased and antialias filters tend to falsify amplitudes. In contrast, the minimum-aperture operator (Figure 1b) avoids these problems as its location and size fits the constructively contributing part of the reflection event, thus providing an improved input for a subsequent amplitude-versus-offset (AVO) analysis (Bancroft and Sun, 2003).

Pruessmann et al. (2004) presented a first approach to perform CRS-based AVO analysis in the *unmigrated* time domain. For complex media, a migration prior to AVO analysis might, however, be inevitable. As depth migration is quite sensitive to velocity model errors and costly in terms of inversion, we propose CRS-based AVO analysis in the *migrated* time domain. In addition to the reduced sensitivity to model

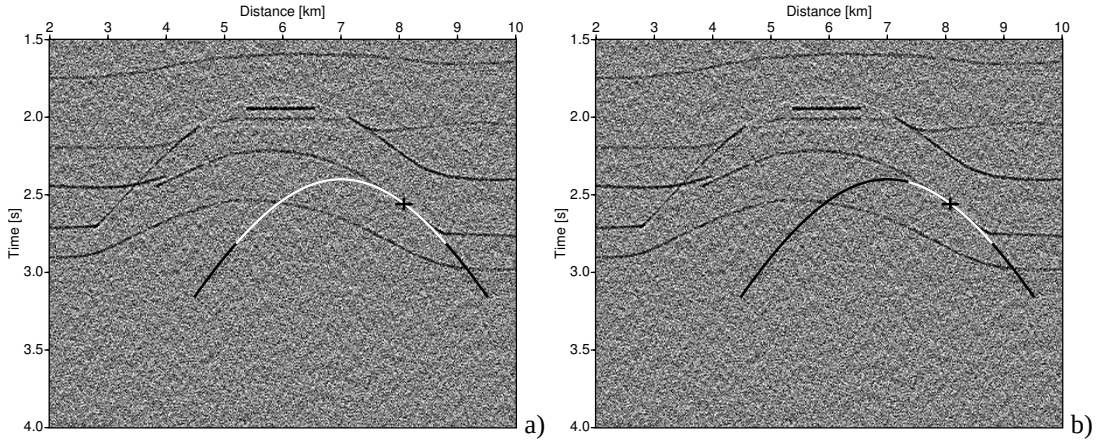

Figure 1: Time migration operator with a) conventional aperture centered around its apex and with b) minimum aperture centered around the stationary point. The respective part of the operator within the aperture is depicted in white.

errors, the time migration benefits from smooth, analytic migration operators and operator slopes; in addition, a consistent, analytic approximation for true-amplitude weight factors can be found, thus avoiding dynamic ray-tracing. Moreover, the time migration velocity model can be obtained in a simple and largely automated manner.

DETERMINATION OF THE MINIMUM APERTURE

The determination of the minimum migration aperture consists of two tasks: the constitution of the stationary point that defines the center for the migration aperture and the size of the projected Fresnel zone which determines its horizontal extension. The basic concept has been described in Jäger (2005) and is briefly reviewed here.

Basics of CRS stack

The CRS method is based on a second-order approximation of the kinematic reflection response of an arbitrarily curved reflector segment in depth. This approximation can be entirely expressed in terms of so-called kinematic wavefield attributes defined at the acquisition surface rather than in the subsurface. In 2D, the commonly used hyperbolic approximation reads (see, e. g., Schleicher et al., 1993)

$$t^2\left(x_{\mathrm{m}},h\right)=\left[t_0+\frac{2\,\sin\alpha\,(x_{\mathrm{m}}-x_0)}{v_0}\right]^2+\frac{2\,t_0\,\cos^2\alpha}{v_0}\left[\frac{(x_{\mathrm{m}}-x_0)^2}{R_{\mathrm{N}}}+\frac{h^2}{R_{\mathrm{NIP}}}\right]. \tag{1}$$

It describes the traveltime along a paraxial ray characterized by source/receiver midpoint x_{m} and half-offset h in terms of the traveltime t_0 along the central normal ray emerging at x_0, the near-surface velocity v_0, and the wavefield attributes α, R_{NIP}, and R_{N}. The latter three are related to the propagation direction and wavefront curvatures of two hypothetical waves, namely the so-called NIP and normal wave, respectively (Hubral, 1983).

Similar to a conventional stacking velocity analysis, the optimum wavefield attributes for each location (x_0,t_0) are determined automatically by means of coherence analysis. Note, however, that this analysis is carried out with a spatial operator in a multi-dimensional parameter domain. The final results are entire sections of the wavefield attributes α, R_{NIP}, and R_{N}, as well as coherence section. For details see, e. g., Jäger et al. (2001).

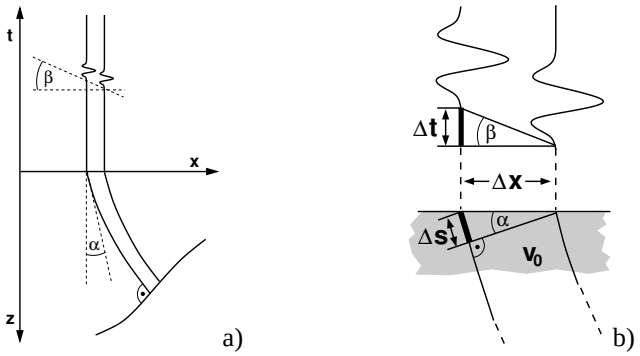

Figure 2: Relationship between emergence angle α of the ZO ray and the local slope β of the associated event in the ZO time section (Figure taken from Jäger, 2005).

Determination of stationary points

In Kirchhoff migration, the main contribution to the diffraction stack stems from the region where the reflection event is tangent to the migration operator, the so-called stationary point x_0. As the CRS operator (1) is already tangent to an reflection event in the data, this tangency condition can be directly evaluated by a comparison of the CRS operator slope and the migration operator slope. The searched-for slope β of the ZO reflection event is related to the emergence angle α of the ZO ray via the near-surface velocity v_0 as can be seen from Figure 2:

$$\tan\beta = \frac{2}{v_0}\sin\alpha\,. \tag{2}$$

For time migration with straight rays as considered here, the migration operator as well as its derivatives are given by analytic expressions. In practice, the modulus of the difference between these two slopes is calculated and the location of the minimum is chosen as stationary point. The associated coherence values help to decide whether the stationary point is reliable by applying a user-given threshold.

The concept of the *Common-Reflection-Point (CRP) trajectory* allows to extrapolate the stationary point to finite offset. Its projection onto the acquisition surface reads (Höcht et al., 1999):

$$x_{\mathrm{m}}(h) = x_0 + r_{\mathrm{T}}\left(\sqrt{\frac{h^2}{r_{\mathrm{T}}^2}+1}-1\right)\,, \tag{3a}$$

with

$$r_{\mathrm{T}} = \frac{R_{\mathrm{NIP}}}{2\,\sin\alpha}\,. \tag{3b}$$

This approximation provides a superior reference for the center of the migration aperture compared to the conventional approach which ignores the deviation between CMP and CRP gathers.

Determination of the size of the projected Fresnel zone

The final information relevant for minimum migration apertures which can be gained from the attributes is the size of the projected ZO Fresnel zone W_{F}. In terms of CRS attributes, it can be approximated as (see, e. g., Mann, 2002)

$$\frac{W_{\mathrm{F}}}{2} = |x_{\mathrm{m}} - x_0| = \frac{1}{\cos\alpha}\sqrt{\frac{v_0\,T}{2\left|\frac{1}{R_{\mathrm{N}}}-\frac{1}{R_{\mathrm{NIP}}}\right|}}\,, \tag{4}$$

where T denotes some measure of the wavelet length. In general, the Fresnel zone size is expected to widen with offset. Unfortunately, this effect is hard to quantify as the velocity model together with the

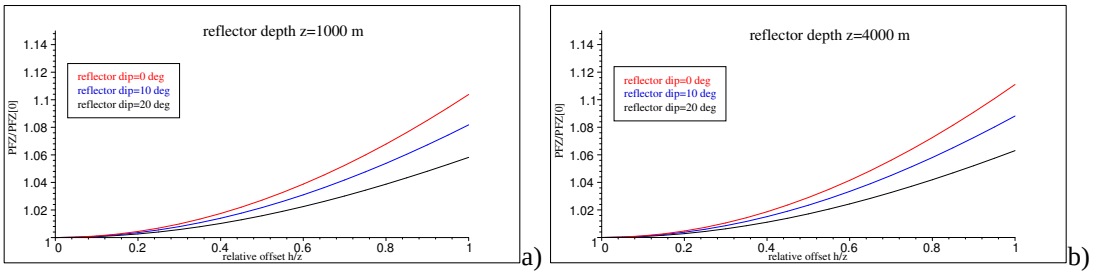

Figure 3: Relative size of the Fresnel zone $W_{\mathrm{F}}(h)/W_{\mathrm{F}}(0)$ over relative offset h/z for a plane interface with dip $0°$, $10°$ and $20°$ beneath a homogeneous overburden. The reflector is located at a depth of (a) $z = 1000\,\mathrm{m}$ and (b) $z = 4000\,\mathrm{m}$.

dip and curvature of the reflector has to be considered. However, forward calculated examples suggest that the widening effect is very small as can be seen from Figure 3: for two analytical models with different reflector depths the relative size of the Fresnel zone $W_{\mathrm{F}}(h)/W_{\mathrm{F}}(0)$ is determined for three different reflector dips. As long as the the offset does not exceed the reflector depth, the relative widening is smaller than $10\,\%$. For practical application, the ZO Fresnel zone size as determined from the CRS attributes is always extended by a certain percentage (usually 10 to $20\,\%$ depending on the attribute quality) as it is crucial not to underestimate the Fresnel zone for true-amplitude processing. Thus, the small widening effect is already covered and may be neglected therefore. For the data example below, the Fresnel zone was set constant for all offsets, an approximation which appears to be reasonably accurate to obtain reliable amplitudes.

GENERAL WORKFLOW

A general workflow for CRS-based minimum aperture time migration is depicted in Figure 4: The CRS stack is applied to simulate a ZO section in a fully automated way. More relevant in this context are the CRS wavefield attribute sections and the associated coherence section. Applying an event-consistent smoothing (Mann and Duveneck, 2004) to the found attributes guarantees a smooth input for the following processing steps. This point is especially important for the determination of the ZO projected Fresnel zone and the stationary point as outliers and unphysical fluctuations might locally introduce some artifacts in the amplitudes.

Based on the coherence values which indicate the location of the reflection events and the reliability of their wavefield attributes, an automated picking process was employed to extract the wavefield attributes along the reflection events. These attributes are then used

- to determine the stationary points for ZO,
- to extrapolate the stationary points to finite offset,
- to estimate the projected ZO Fresnel zone, and
- to calculate time-migration velocity values.

In order to determine the time-migration velocity values, the CRS wavefield attributes for one ZO location $P_0 = (x_0, t_0)$ have to be mapped into the apex of the corresponding time migration operator. As the NIP wave does not depend on the reflector curvature and orientation, it allows to approximate the ZO diffraction response of a diffractor located on the (unknown) reflector segment in depth. Expressing the CRS diffraction response in apex coordinates allows to establish a relationship between the searched-for RMS velocity defined at the operator apex and the original CRS attributes (Mann, 2002).

Each set of (reliable) CRS attributes can now be related to a migration velocity value and its corresponding location in the time domain. In a subsequent infill procedure, the migration velocities are inter- and extrapolated using a distance weighted polynomial interpolation. This approach has, so far, no sound physical justification.

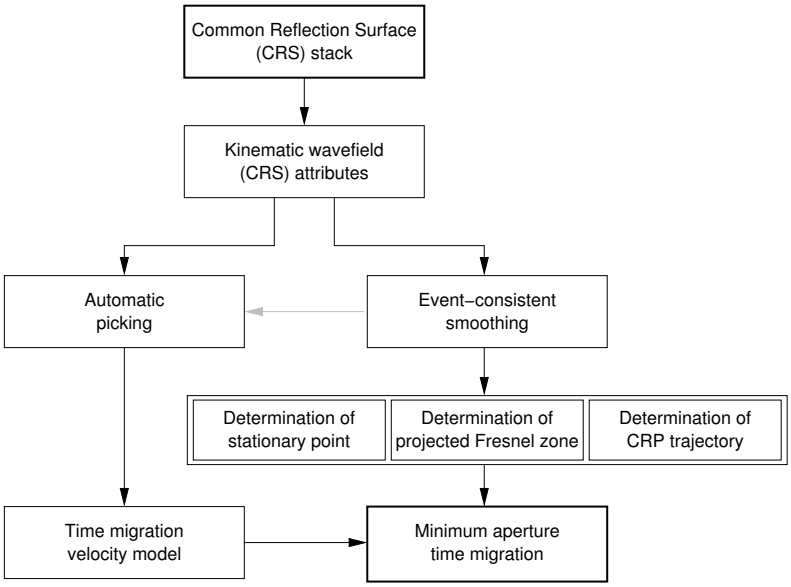

Figure 4: General workflow for CRS-based limited aperture time migration. The CRS attributes serve as input for the determination of the migration attributes (stationary point, minimum aperture, and CRP-trajectory) and the time migration velocity model.

SYNTHETIC DATA EXAMPLE

To demonstrate the potential of the true-amplitude CRS-based Kirchhoff time migration for AVO analysis we generated a synthetic prestack data set for the model shown in Figure 5a. The target region for the amplitude extraction is the horizontally layered structure beneath the uppermost dome-like interface. The elastic parameters are chosen such as to mimic a sequence of gas/oil/water contacts. The primary P-waves have been modeled by means of a wavefront construction method using a zero-phase Ricker wavelet with a dominant frequency of 40 Hz. Edge diffractions have not been considered. Colored noise was added; a representative common-offset section is shown in Figure 6.

The interpolated smooth time-migration velocity model is shown in Figure 5b. The model is kinematically consistent with the data as can be seen from the set of common-image gathers (CIGs) displayed in Figure 7.

The time migration was performed twice: on the one hand in a conventional way with user-given aperture, on the other hand with the minimum aperture given by the (extrapolated) projected Fresnel zone. The user-given aperture was chosen such that the steep flanks of the dome-like structure have been imaged. The projected ZO Fresnel zone is shown in Figure 8 for those locations where stationary points have been detected. As expected, its size increases with increasing traveltime and increasing curvature of the reflection events.

Stacks of the two true-amplitude prestack migration results are depicted in Figure 9. For Figure 9b, the minimum-aperture migration was only performed at locations where stationary points have been detected. This removes many of the artifacts due to modeling deficiencies, but might cause gaps in regions with conflicting dips (e. g. at the flanks of the dom-like structure) or on weak events (e. g. on the lower-most reflector between $x = 7$ km and $x = 8$ km). In practice, the user-given aperture is used at all other locations to obtain a fully covered image without gaps.

Finally, the amplitudes for the target reflectors have been extracted. Figure 10 shows the AVA curves for one selected common image gather for both aperture definitions applied to the noisy data. In addition, the minium-aperture migration has been applied to the same data without noise to obtain reference values. Obviously, the CRS-based results are closer to the reference values and far more contiguous compared to their conventional counterparts. For each target reflector, the extracted amplitudes have been used to

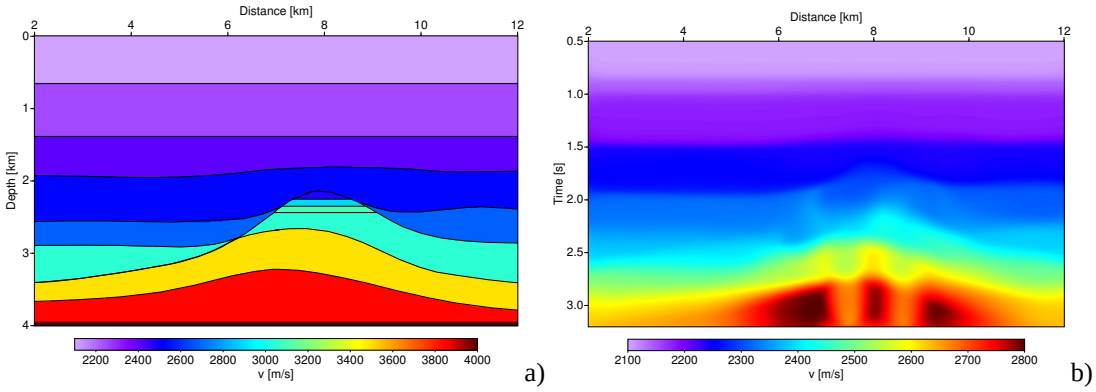

Figure 5: a) Interval P-wave velocity model used to generate the synthetic data, b) time migration velocity model determined from CRS wavefield attributes. Note the different color scales.

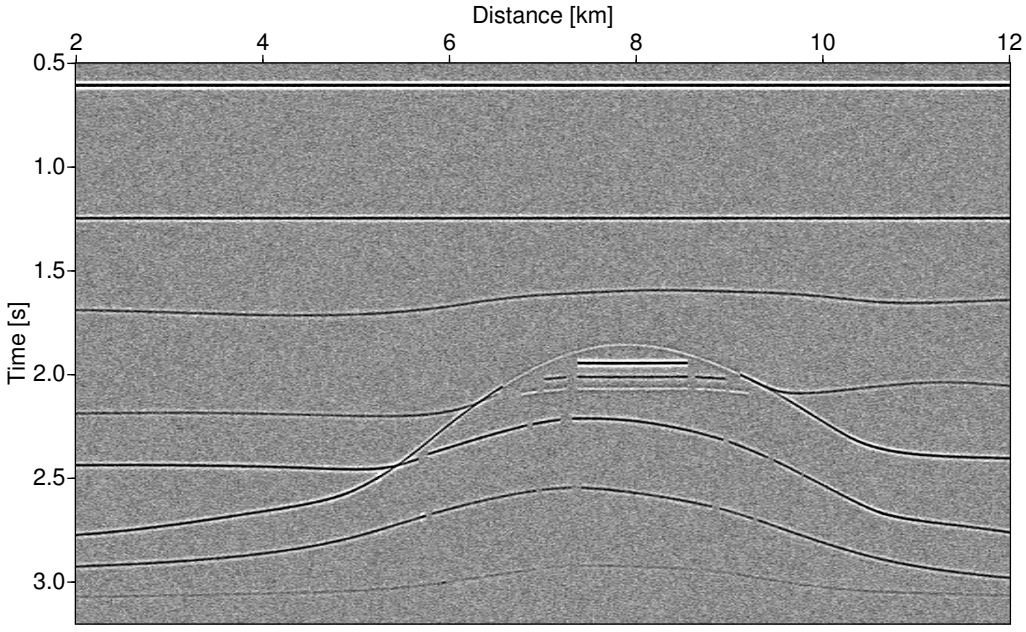

Figure 6: Representative common-offset section ($h = 100\,\mathrm{m}$) extracted from the synthetic prestack data.

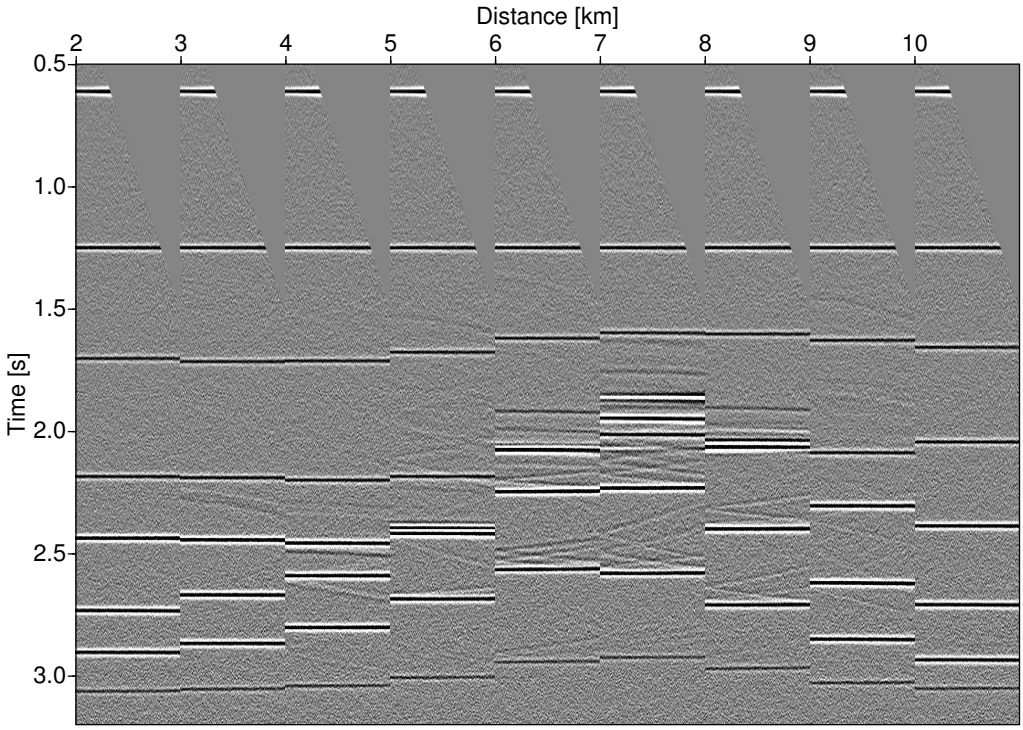

Figure 7: Several common-image gathers extracted from the time-migrated prestack data.

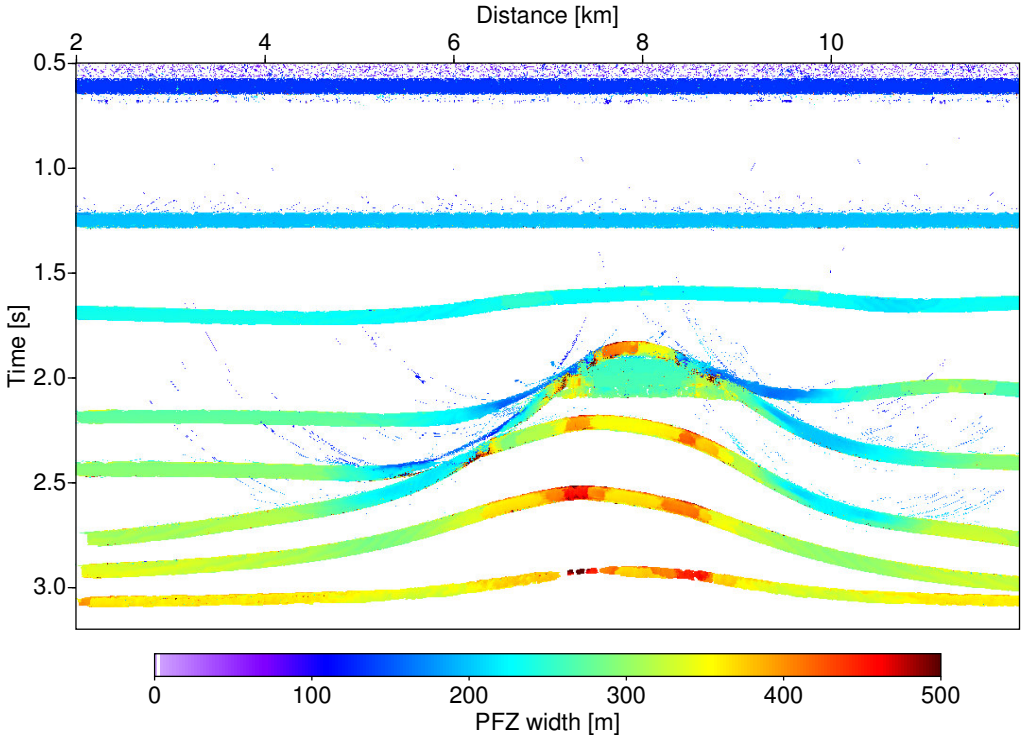

Figure 8: Size of projected first ZO Fresnel zone estimated from the CRS attributes. Only locations with identified stationary points have been considered.

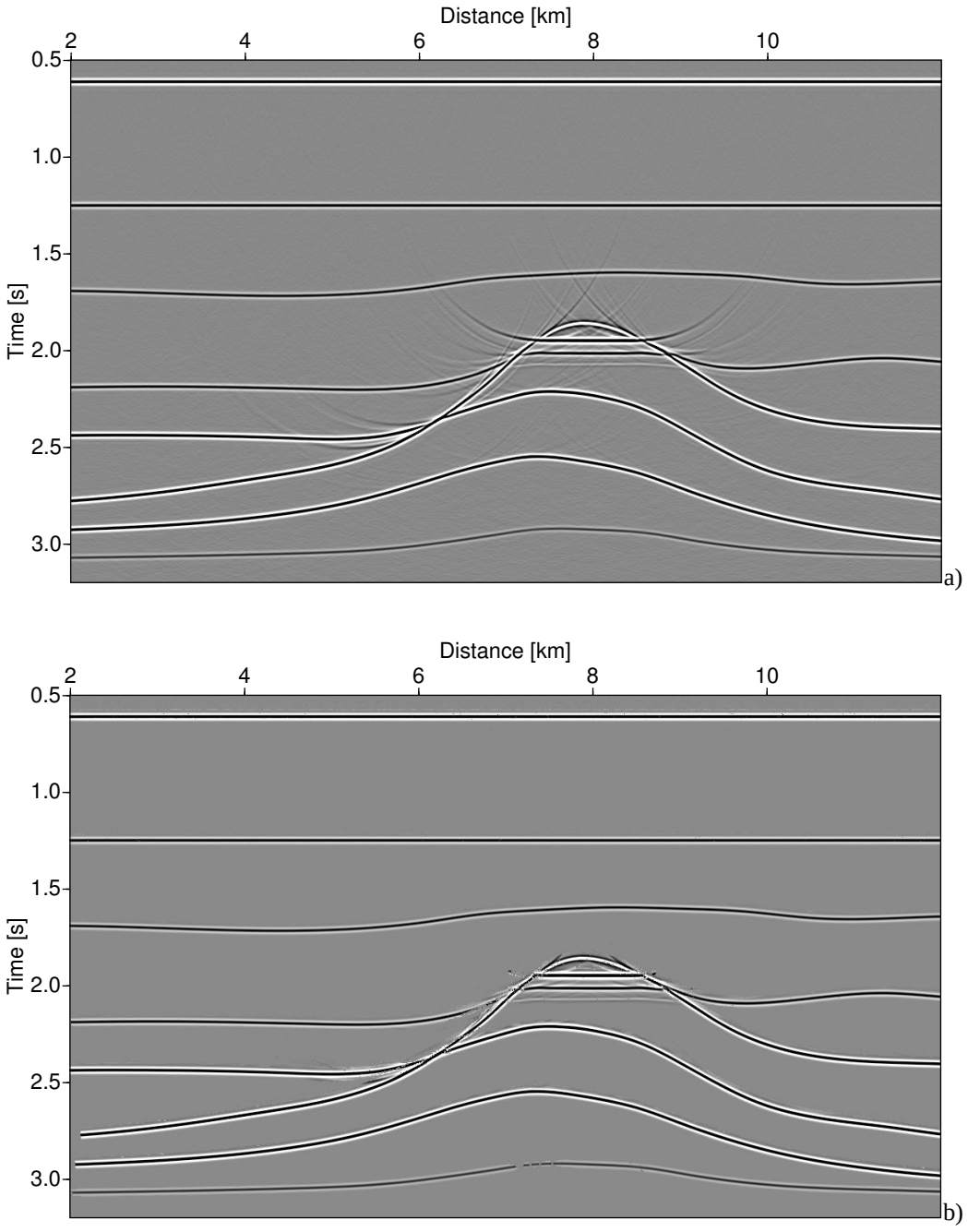

Figure 9: Stacks of the time-migrated prestack data with a) conventional user-defined aperture and b) CRS-based minimum-aperture. In the latter case, only locations with identified stationary points have been considered. The artifacts mainly visible in the conventional result are due to missing edge diffractions and gaps in the modeled prestack data.

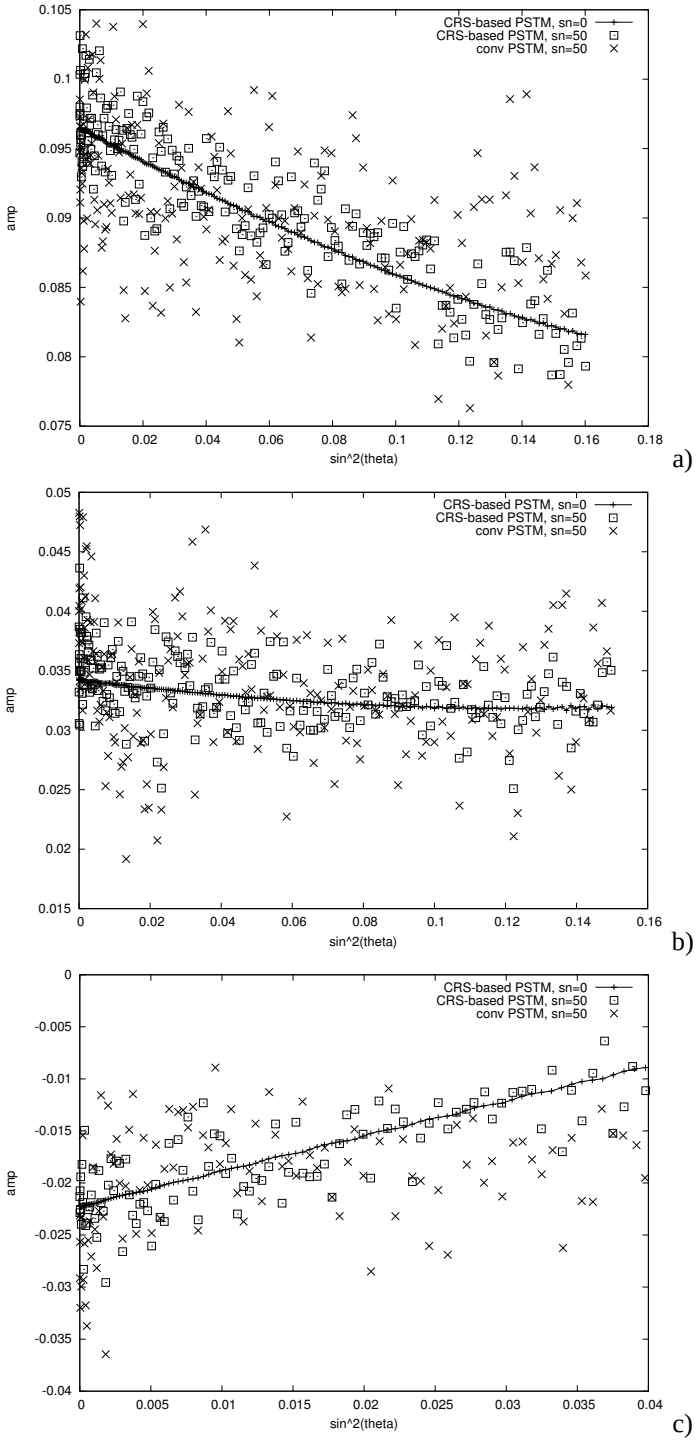

Figure 10: Amplitudes along the a) first, b) second, and c) third target reflector extracted from the time-migrated prestack data for one selected CIG. The linepoints denote the reference curve obtained for the same dataset without noise. Note the significant differences in dispersion between the CRS-based and the conventional result.

generate a horizon-based AVO crossplot (Figure 11) using a stable linear regression method Walden (1991). Again, the noise-free dataset was used to obtain reference values. In general, the migration results for the noisy data show an oval distribution of the points around these reference values depending on the S/N ratio of the considered reflector (which is decreasing from the first to the third target reflector). If migration artifacts or different events contribute to the diffraction stack, a trend might be introduced in the crossplot or the linear regression might even totally fail. Due to the decreased noise-level in the amplitudes, the CRS-based results show less dispersion and give an overall better estimation of the reference values.

CONCLUSIONS

Jäger (2005) successfully applied CRS wavefield attributes to estimate the location of stationary points and the projected Fresnel zone required for minimum-aperture Kirchhoff depth migration. We demonstrated that this CRS-based minimum aperture concept can be transferred back to the time domain. Here, not only the sensitivity to model errors is reduced, but also the time migration velocity model building can be performed in a highly automated and simple way. The entirely analytic migration operators and their corresponding derivatives allow an efficient implementation, especially concerning the determination of stationary points.

Due to the reduced sensitivity to model errors and the optimum migration aperture we obtain more reliable amplitudes for AVO/AVA analyses compared to conventional approaches.

OUTLOOK

As future improvement, a physically sound model infill procedure should be incorporated. Furthermore, the extrapolation of the projected Fresnel zone to finite offset has to be investigated in more detail. An extension of the approach to 3 D is expected to increase the benefit of the method as the efficiency of Kirchhoff time migration will be of significant importance.

ACKNOWLEDGMENTS

This work was kindly supported by the sponsors of the *Wave Inversion Technology (WIT) Consortium*, Karlsruhe, Germany.

REFERENCES

Bancroft, J. and Sun, S. (2003). Fresnel zones and the power of stacking used in the preparation of data for AVO analysis. In *Expanded abstracts, 73rd Ann. Internat. Mtg.*, pages 231–234. Soc. Expl. Geophys.

Höcht, G., de Bazelaire, E., Majer, P., and Hubral, P. (1999). Seismics and optics: hyperbolae and curvatures. *J. Appl. Geoph.*, 42(3,4):261–281.

Hubral, P. (1983). Computing true amplitude reflections in a laterally inhomogeneous earth. *Geophysics*, 48(8):1051–1062.

Jäger, C. (2005). Minimum-aperture Kirchhoff migration by means of CRS attributes. In *Extended abstracts, 66th Conf.* Eur. Assn. Geosci. Eng. Session F042.

Jäger, R., Mann, J., Höcht, G., and Hubral, P. (2001). Common-Reflection-Surface stack: image and attributes. *Geophysics*, 66(1):97–109.

Mann, J. (2002). *Extensions and applications of the Common-Reflection-Surface Stack method*. Logos Verlag, Berlin.

Mann, J. and Duveneck, E. (2004). Event-consistent smoothing in generalized high-density velocity analysis. In *Expanded Abstracts, 74th Ann. Internat. Mtg.* Soc. Expl. Geophys. Session ST 1.1.

Pruessmann, J., Coman, R., Endres, H., and Trappe, H. (2004). Improved imaging and AVO analysis of a shallow gas reservoir by CRS. *The Leading Edge*, 23(9):915–918.

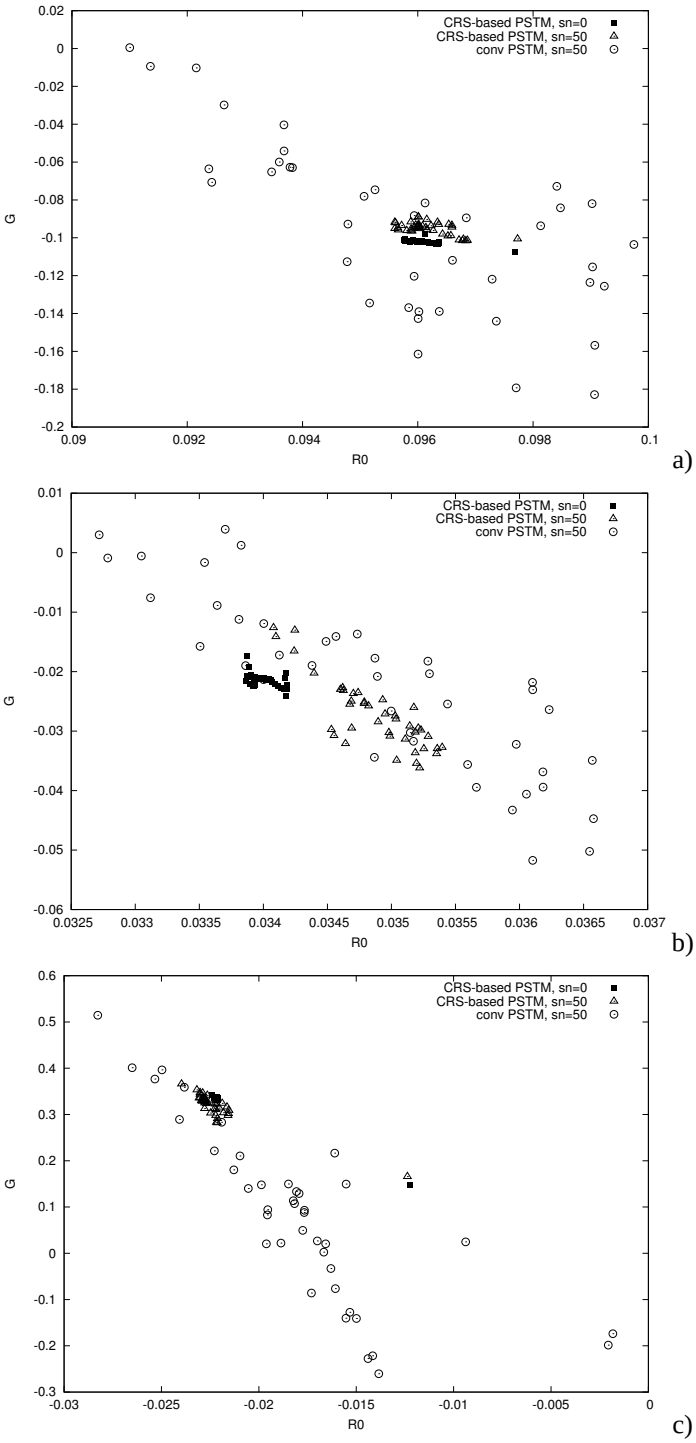

Figure 11: Horizon-based crossplot obtained for the a) first, b) second, and c) third target reflector. Again, the result from the noise-free datasets determines the reference values.

Schleicher, J., Hubral, P., Tygel, M., and Jaya, M. S. (1997). Minimum apertures and Fresnel zones in migration and demigration. *Geophysics*, 62(1):183–194.

Schleicher, J., Tygel, M., and Hubral, P. (1993). Parabolic and hyperbolic paraxial two-point traveltimes in 3D media. *Geophys. Prosp.*, 41(4):495–514.

Walden, A. T. (1991). Making AVO sections more robust. *Geophys. Prosp.*, 39:915–942.